A Study of High Power Pulsed Characteristics of Low-Noise GaAs MESFET's

DAVID S. JAMES, MEMBER, IEEE, AND LESLIE DORMER

Abstract—Low-noise GaAs MESFET's of various types have been investigated for short-term catastrophic burnout ratings when exposed to pulses from an *X*-band radar transmitter 6=T/R cell combination. Failure modes have been categorized, and SEM, EDAX, and optical techniques employed in the associated failure analyses. A limited number of longer term tests at lower pulse levels are also described. Post-dosage and interpulse RF performance has been studied by use of a special test set described, and the initial results obtained are presented.

I. Introduction

THIS PAPER describes a study of some important reliability and performance aspects of GaAs low-noise MESFET's when used under pulsed conditions. The main motivation for this is the assessment of the suitability of FET preamplifiers for use in radar receivers, where the amplifier is subjected to pulses from the T/R protection unit. Typically a primed T/R-limiter protector produces pulses consisting of a fast, roughly triangular RF spike component having energy of the order of 10 nJ (~3-ns half-width, ~3.5-W peak) followed by a longer flat leakage component having a level of the order of 100 mW. It was suspected that, in comparison with parametric amplifiers, FET preamplifiers would be relatively fragile under such conditions. Relatively little relevant work has been reported so far [1]–[4], and it is considered important that these aspects be adequately investigated in order that radar FET amplifier requirements may be properly addressed, without prejudice to system reliability. In particular, the interpulse performance of such devices is critical to correct radar operation.

The work described here is incomplete, but includes new information on the following aspects:

a) short-term catastrophic burnout testing of various devices;
b) associated failure investigations;
c) longer term tests under representative lower level pulsed conditions;
d) interpulse and post-dosage recovery phenomena.

Manuscript received April 13, 1981; revised August 10, 1981. This work was supported in part by the United Kingdom Ministry of Defence (Procurement Executive, D. CVD).

These authors are with the Microwave Division, Ferranti Electronics Limited, Poynton, England.

II. Catastrophic Burnout

A. Test Procedure

A number of devices have been subjected to short term exposure to pulsetrains from an *X*-band magnetron transmitter followed by a primed T/R cell which was specially tailored to provide relatively high output levels. The overall test procedure used is shown in Fig. 1. Prior to subjecting the devices to a program of controlled RF exposure each unit is dc tested (reverse leakage, transconductance, $\log i/\log v$). Included in the measurement arrangement is an automatic noise figure meter, with associated manual RF switches such that the system noise figure can be measured from a period of approximately 3 s after termination of each 4-min dose. Doses of increasing energy level are given until failure; the latter is arbitrarily defined as a) a change in drain current of greater that 20 percent, and/or b) an increase in post-dosage noise figure of greater than 3 dB.

The test arrangement is shown in Fig. 2. The pulsetrains are analyzed and statistically evaluated by means of a computer driven digital transient analyzer. All the RF spike components are of approximately triangular shape, and of 3-ns nom. half-width. Each device is installed in a single-stage amplifier test jig with dedicated constant-voltage power supply circuits which provide good regulation capability and immunity to RFI. Current limiting resistors of 10-Ω and 2-kΩ value are incorporated into the drain and gate supplies, respectively. The RF circuit is arranged to provide approximately the minimum noise measure over the 9.0–9.5-GHz range. For each test, the drain current is monitored continuously. It has been found to decrease monotonically with increasing RF pulse energy, and to typically exhibit a finite recovery time after termination of dosage.

All the devices studied are in hermetically packaged form having gate lengths in the 0.5–1-μm nominal range and of various detailed design configurations and gate metals. Nearly all the devices were procured as standard commercial units, without specification or special screening. (See Table I.)

B. Results

Initial results are presented in bar dot format in Fig. 3. There is considerable variation observed in burnout level

0018-9480/81/1200-1298$00.75 ©1981 IEEE

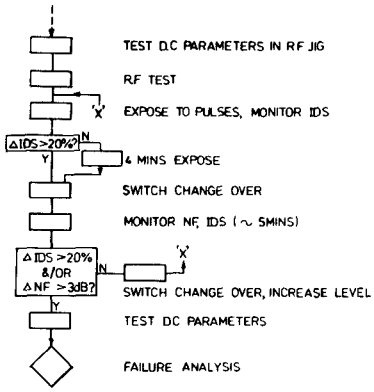

Fig. 1. Test procedure for short-term catastrophic burnout tests.

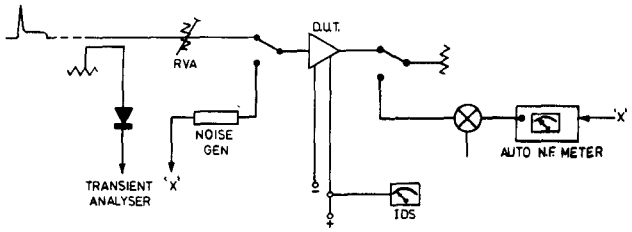

Fig. 2. Test arrangement for catastrophic burnout measurements.

TABLE I
DEVICE TYPES STUDIED—THE LETTER CODE IDENTIFIES THE MANUFACTURER

DEVICE TYPE	GATE METAL	GATE PAD	S/D OHMIC CONTACT	S/D PAD OVERLAY	GATE LENGTH μm	No. OF GATE FEEDS	GLASSIFICATION
A	Al	Ti	Au-Ge	Cr/Pt/Au.	1	1	Yes
A	Al	Ti	Au-Ge	Cr/Pt/Au.	0·5	2	Yes
B	Al	Al	In/Ge/Au.	–	1	2	No
B	Al	Al	In/Ge/Au.	–	0·5	2	No
B	Al	Al	In/Ge/Au.	–	0·5	2	No
B	–	–	–	–	0·5	2	No
C	Au	–	–	–	1	1	No
D	Al	Ti/Pt/Au.	Au-Ge/Pt.	Ti/Pt/Au.	1	1	Yes
D	Al	Ti/Pt/Au.	Au-Ge/Pt.	Ti/Pt/Au.	1	4	No
E	Ti/Cr/ Pt/Au.	Ti/Cr/ Pt/Au.	Au-Ge/ Ni/Au	Ti/Cr Pt/Au.	1	2	Yes
F	Al	–	Au-Ge/Ni	–	1	2	No

ALL GATE WIDTHS ARE 300-500μm. CHANNEL LENGTHS ARE 3-5μm NOMINAL.

between device types, and significantly between batches of the same type. Within a batch of the same type there seems less variation, although insufficient sample size precludes a meaningful statistical description. It is apparent that whereas some devices are sufficiently rugged to withstand spike energies of over 150 nJ, others of the same type are observed to fail after brief exposure to pulses of maximum spike energy of only 8 nJ. Unfortunately the latter figure coincides with the level of energy transmitted from a typical modern protection unit, and constitutes some cause for concern. There is as yet no apparent correlation between these burnout levels and measured dc parameters, although there is limited evidence of correlation with some aspects of cosmetic quality of the device chip, as examined subsequently.

The results shown in Fig. 3 show a greater variation in the values of MAX SPIKE ENERGY (7 nJ to greater than 160 nJ) than the 20-nJ to 50-nJ range for 3-ns duration pulses reported by Whalen *et al.* in [2, fig. 7]. One reason for the difference is that the values shown in Fig. 3 are for *incident* pulse energy, whereas Whalen *et al.* show values for *absorbed* pulse energy. Another reason may be that Whalen *et al.* show data at 3 ns for just 13 MESFET's of 3 types which are all 1.0-μm gate devices. The data in Fig. 3 are for nearly 60 MESFET's of 9 types and subtypes including 1.0- and 0.5-μm gate devices. What is perhaps most interesting is the very high (>160 nJ) max spike energy required to burn out some MESFET's.

In nearly all cases both the above failure criteria were met, i.e., both noise figure and drain current changed significantly on failure. Similarly failure was seen in nearly all cases to be an apparently instantaneous event. In fact,

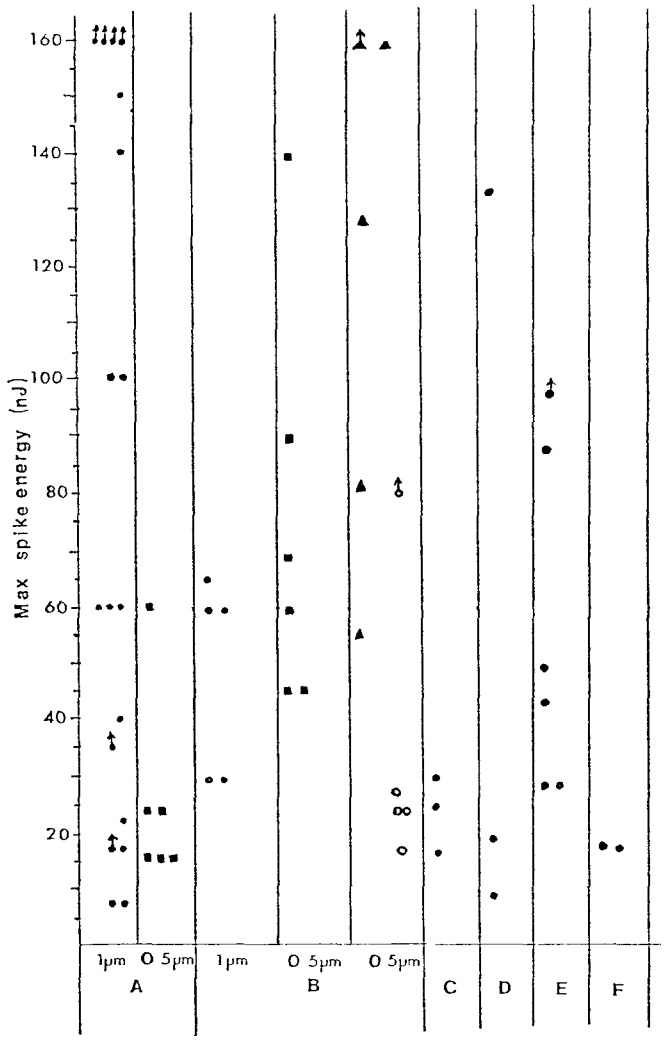

Fig. 3. Initial results from catastrophic burnout tests. The level indicated is the max spike energy incident on the test jig associated with short-term device failure (test procedure per Fig. 1). Primed cell data only is shown, and the arrow indicates the device did not fail at this level.

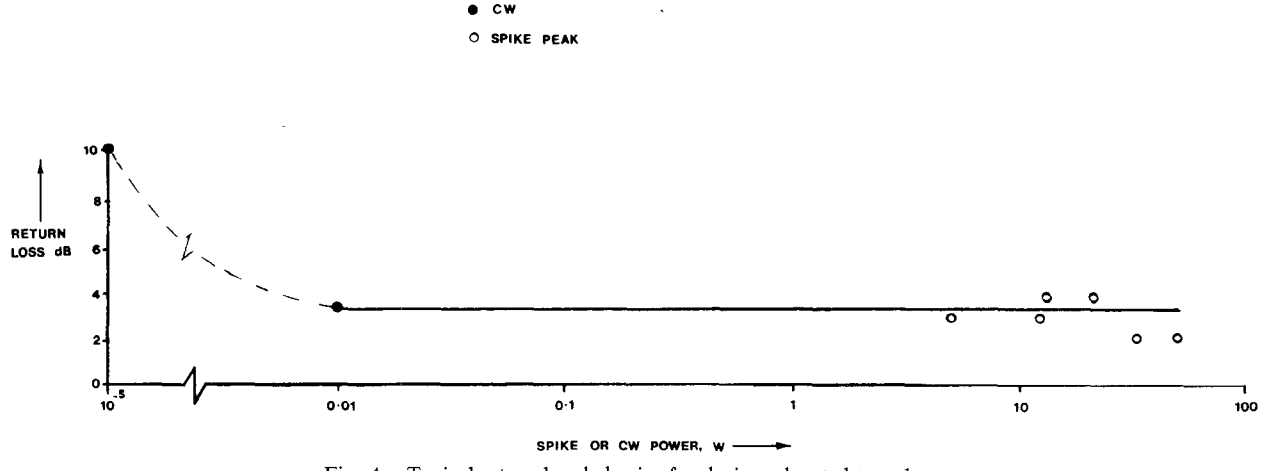

Fig. 4. Typical return loss behavior for device subjected to pulses.

by adjustment of the threshold detector of the transient digitizer it is possible to observe at a conveniently slow rate the behavior associated with each and every one of the most energetic pulses, and under these conditions it appears that the device indeed seems to fail coincident with one such high energy pulse, as evidenced by a significant

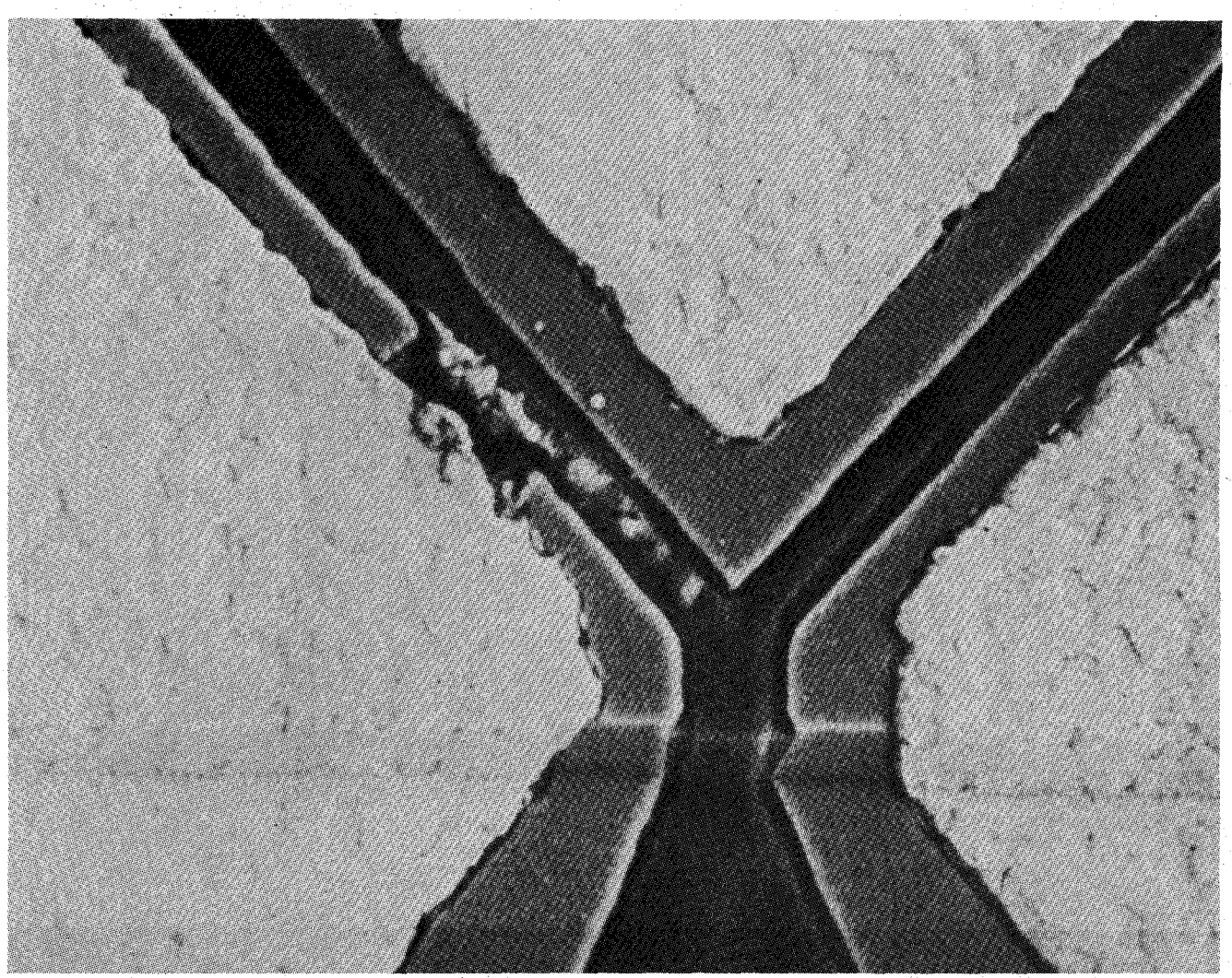

Fig. 5. SEM photograph of typical gate/source short-circuit, the predominant failure mode.

change in drain current. Preliminary, separate CW only tests support the tentative conclusion that it is the large RF spike component which causes burnout.

Typical measured return loss behavior is shown in Fig. 4; the values are of significance in consideration of the dynamic current and voltage at the gate/source junction and its possible relationship to the mechanisms of failure. Some 50 percent of the incident power is reflected at high RF spike powers.

III. Failure Aspects

A. Failure Modes

The catastrophic burnout results reveal gate/source short-circuits as the predominant mode of electrical failure. In order of frequency of occurrence the five identified failure modes are:

a)	gate/source short circuit	~60 percent of failures
b)	low transconductance	~20 percent of failures
c)	drain/source short circuit	~10 percent of failures
d)	reduction to an abnormally low drain current	~5 percent of failures
e)	increase in noise figure	<5 percent of failures.

For the dominant failure mode a), metal migration is the cause, as explained further below. Typically the saturated drain current I_{DSS} remains essentially unchanged. In many cases there remains after failure some degree of transconductance, where sufficient active gate width is still connected and the gate/source resistance remains relatively high. Massive channel damage (MCD) observed by Whalen *et al.* [1], [2] for these very short spikes does not appear, in this context, to be such a significant factor in the tests reported here.

For the second most common failure mode the I_{DSS} value usually remains unchanged, but the transconductance degrades, due to a break in the gate width. Clearly the delineation between the two categories is sometimes blurred when the details of the specific failure analyses are examined.

B. Failure Analysis

Failure analyses have been performed on all devices, using at least optical, SEM, and EDAX techniques. A small percentage of burnout failures were due to faulty device manufacture involving one or more of the following irregularities: a) untidy or deficient packaging, b) irregular

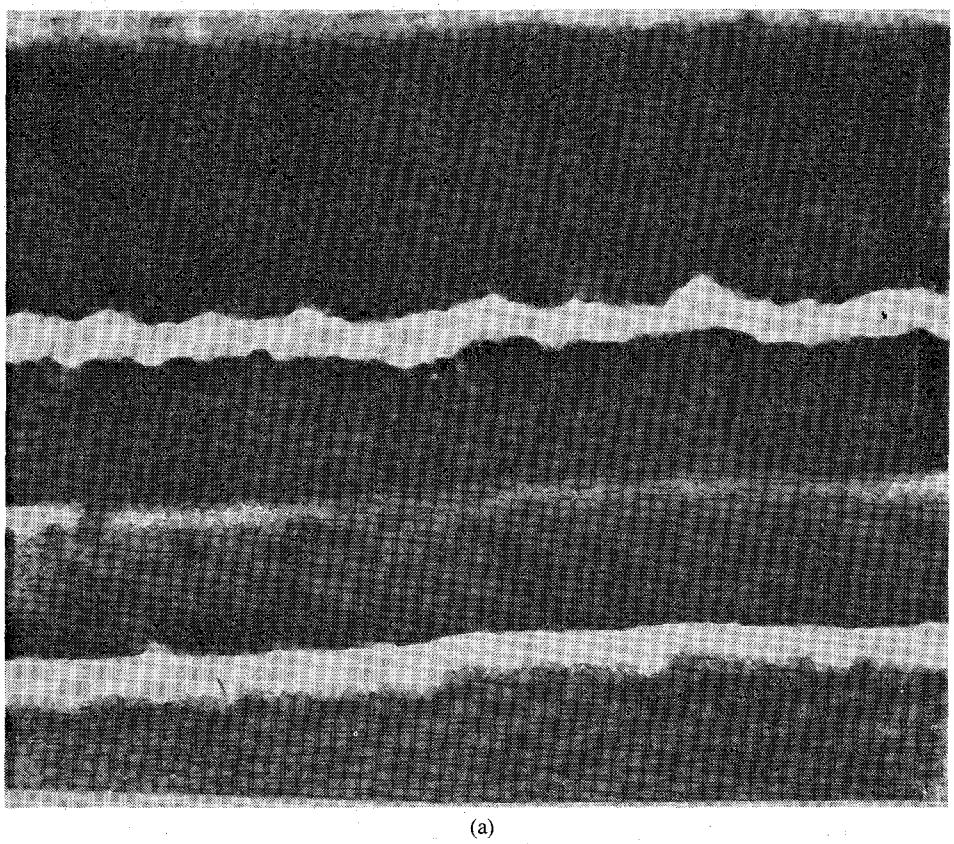

(a)

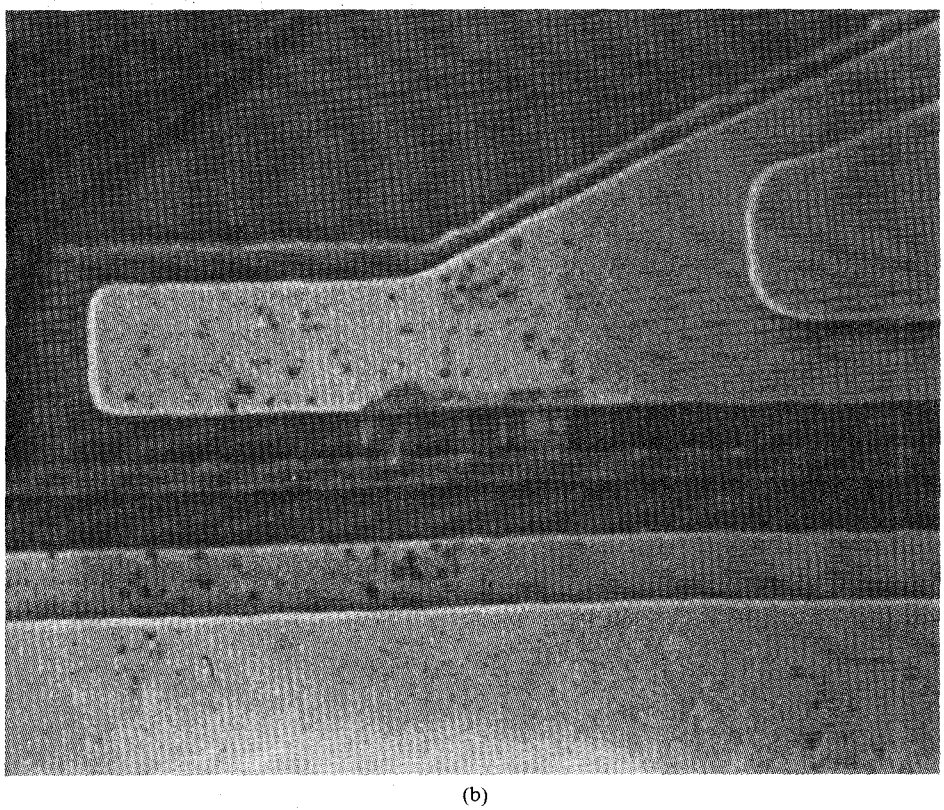

(b)

Fig. 6. (a) SEM photograph of gate/source metal migration (short-circuit). (b) Similar to Fig. 6(a) but adjacent to gate entry.

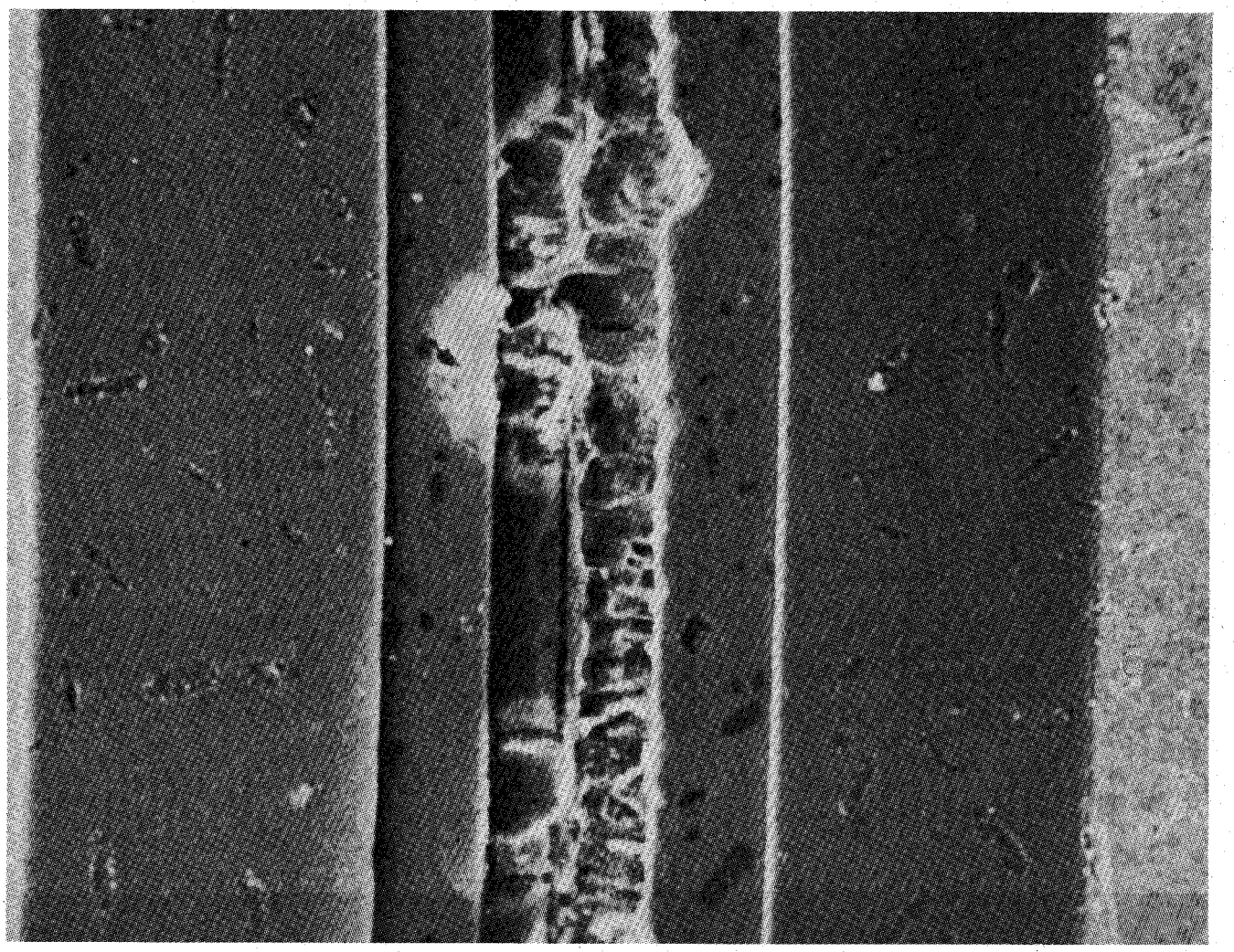

Fig. 7. Massive channel damage example.

gate definition, and c) misaligned gates. In a majority of cases, however, it has not been possible to determine a failure mode which is common to all the devices, or even to one type of device or to specific batches of a type. It is considered that exitaxial and Schottky contact imperfections are most likely causes, wherein stressing brings about a temperature increase in extremely localized spots; depending upon the extent of the sensitized area the failure mechanism proceeds as either surface metal migration, or an interaction of material at deeper level, resulting in the now familiar eruption of the gate/source or gate/drain channel (Fig. 5).

SEM examination has been the most useful technique for detailed categorization and study of the different defects. These are:

a) metal migration:
   1) gate/source or gate/drain channel;
   2) gate entry adjacent to step;
b) gallium arsenide melt down and eruption:
   1) full width of gate/source or gate/drain channel;
   2) localized spots in gate/source or gate/drain channel;
   c) step damage;
   d) overheating.

Fig. 5. illustrates behavior associated with the predominant failure mode, gate/source short-circuit.

Metal migration is evidenced in the example shown in Fig. 6(a). This is fairly subtle; more often for this failure mode we observe a more dramatic effect, the source metal identifiable as the striations or areas of lighter material in the channel. There is some correlation between gate stripe irregularity and the site of the activity, attributable to high field behavior. A more pronounced example of this is shown in Fig. 6(b). which also demonstrates the tendency, in all types studied, for the failure site for gate/source shorts to be adjacent to the gate entry.

Massive channel damage (MCD [1]–[2]) along the whole gate/source region is revealed in Fig. 7. It is to be noted also that there is some damage to the drain.

As an example of GaAs meltdown and eruption Fig. 8. is presented. This is a classic example of gate/source blowout, attributed under normal circumstances to electrostatic discharge damage [3]. The clearly visible bridge is, as proved by EDAX study, once-molten active layer GaAs,

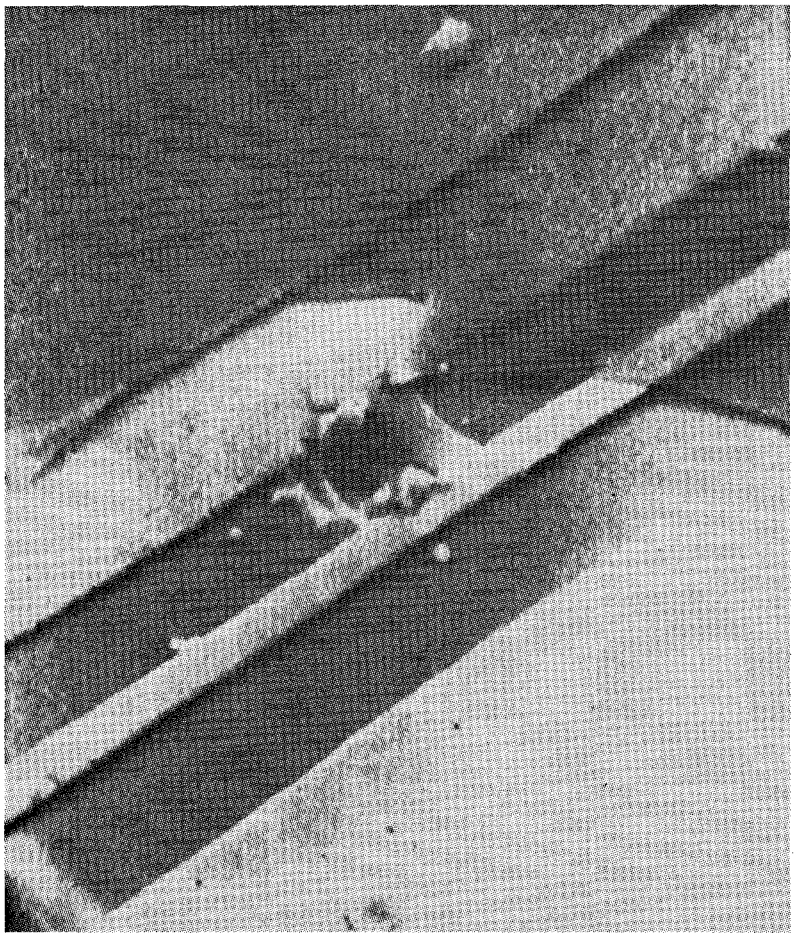

Fig. 8. GaAs meltdown and eruption. The bridge is of once-molten active layer GaAs, *not* metal, as proved by EDAX examination. Also shows cracked and displayed glassification overlay.

not metal. This characteristic is consistent with the experience of Whalen *et al.* [1], [2]. Unlike the latter authors, however, we have found that this type of failure is dominant not just for device types E and D, but also for types B and others. Where device glassification is used, the overlay is normally found to be cracked and often portions completely displaced, as in Fig. 8, or peeled backwards, as in Fig. 9.

Fig. 9. is also an extremely dramatic example of gate damage at the mesa step. This is the most extensively damaged example seen of this type. There is evidence of very high temperature having occurred, and the step has been completely destroyed.

A less dramatic example of overheating damage is shown in Fig. 10(a). There is evidence of alloying of the gate metallization, in this particular case gold, with the substrate material, and for this sort of investigation the technique of low-angle ($\sim 6°$ taper) sectioning has been applied. Fig. 10(b) reveals the depth of damage under the gate pad metal, and in the region of the gate entry, for the same device recorded prior to lapping in Fig. 10(a). This example is for the predominant failure mode, gate/source short-circuit.

A further example of the power of the taper lapping technique is revealed in Fig. 11, showing that processing difficulties would appear to give rise to the possibility that one claimed advantage of the recessed-gate structure, i.e., reduction of interelectrode field, may be negated.

EDAX techniques have been found useful in identifying materials at different locations after failure. One blowout examined under EDAX is shown in Fig. 12, revealing that there has been considerable temperature excursion, as evidenced by the disassociation of Ga and As, and of Au and Ge. The whole failure process appears to have been volcanic, as material is thrown out in disassociated form. The elements found are overlayered on the photograph.

IV. Longer Term Pulsed Exposure

A limited number of 0.5- and 1-μm devices of type A have been subjected to longer term exposure under conditions which correspond closely to actual radar use. The amplifiers were exposed to pulses from a representative magnetron/primed T/R-limiter combination for periods of up to 1 000 h. Four 0.5-μm devices successfully survived the 400-h test period. Of the dozen 1-μm devices tested, one failure was experienced after approximately 100 h, one

Fig. 9. Gate step failure; most dramatic example yet seen. Also shows peeled glassification overlay.

after 300 h and one after 620 h, even though the 6-nJ max. spike energy at the input was around an order of magnitude below the average short term burnout level recorded (See Fig. 3). There is thus suspicion of either a cumulative wearout mechanism or of a greater statistical probability of occasional very high spike energies than though likely to emanate from the protection unit. Support for either possibility is provided by tests on one further device of this same type; although the unit survived the normal 4-min dosage of 60-nJ max. spike energy, it subsequently failed after approximately 1-h exposure at this same level. Those devices which did not fail catastrophically exhibited less than 0.15-dB change in gain or noise figure at the end of the test period. This apparent paradox is similar to the situation encountered with mixer diodes utilized under like conditions.

To examine these aspects further, the special test set described below is now being used. This incorporates a solid-state pulse source which drastically reduces the statistical variation in pulse energies incident on the test device, and will shortly resolve whether such failures are due to a cumulative effect or to the occasional very large pulse.

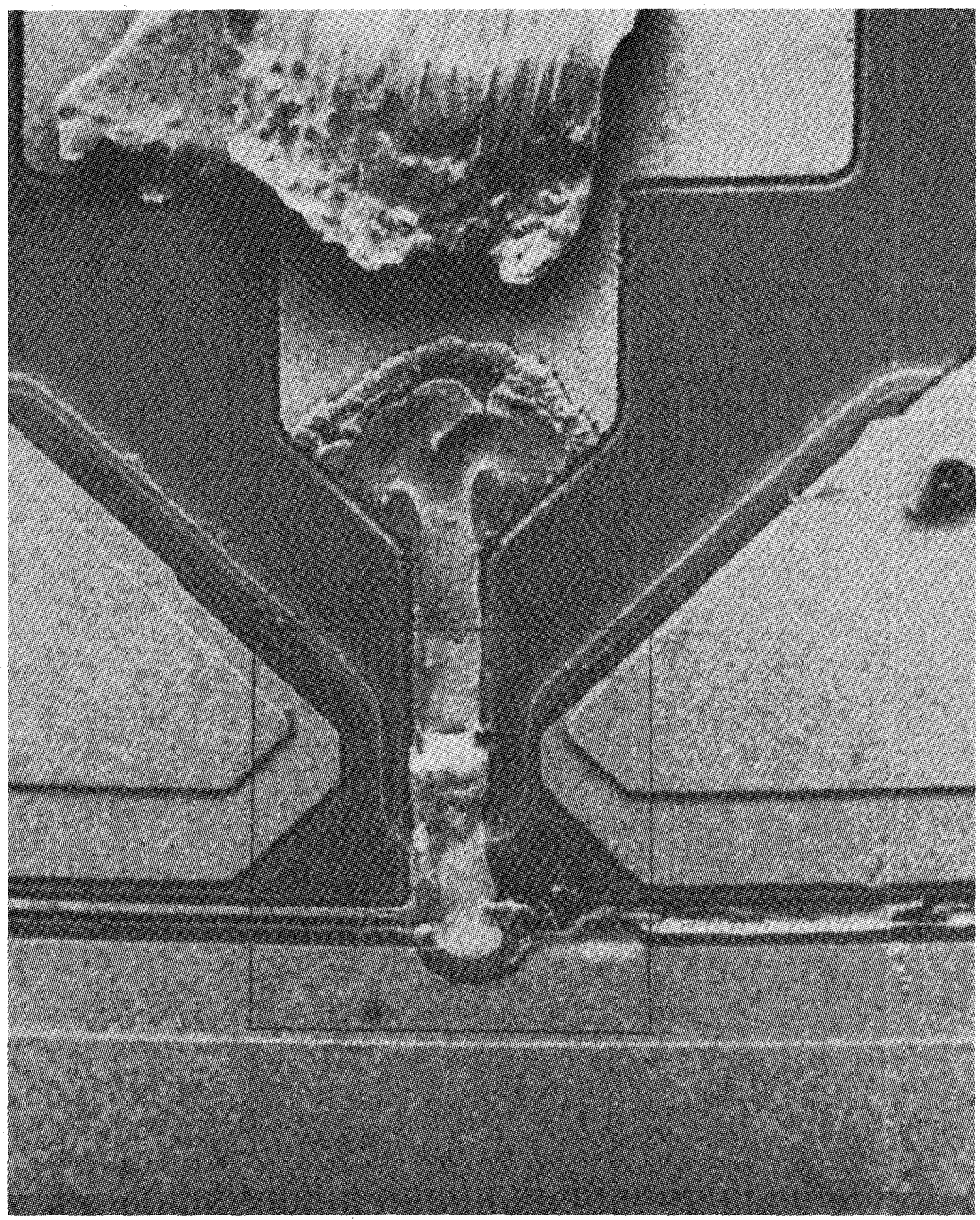

(a)

Fig. 10. (a) Overheating of gate entry area, and gate/source short.

We have already tentatively concluded (Section II-B) that failure appears to occur upon incidence of a single large spike, at least in the case of short-term exposure.

V. Noncatastrophic Effects

A. Post-Dosage

For many devices subjected to the program of controlled short-term dosage (Section II-A) the drain current is seen to exhibit a relatively long recovery (increase) to the final value in the period immediately after termination of the 4-min dosage. In all such cases there is a similarly behaved recovery of system noise figure. Typical results are shown in Fig. 13; some of these changes may be attributable to variations in gain, and this is under investigation using the test set described below. In some cases the initial low energy (5–10-nJ max.) dosage results in an apparently permanent change in noise figure, i.e., an annealing effect, usually of the order of 0.1–0.2-dB increase. Some devices have exhibited as much as 1-dB increase in this noise figure as measured approximately 3 s after termination of the pulse exposure, and it is interesting to note that a reasonable percentage of devices showed a recoverable decrease rather than increase in this figure at this point in time.

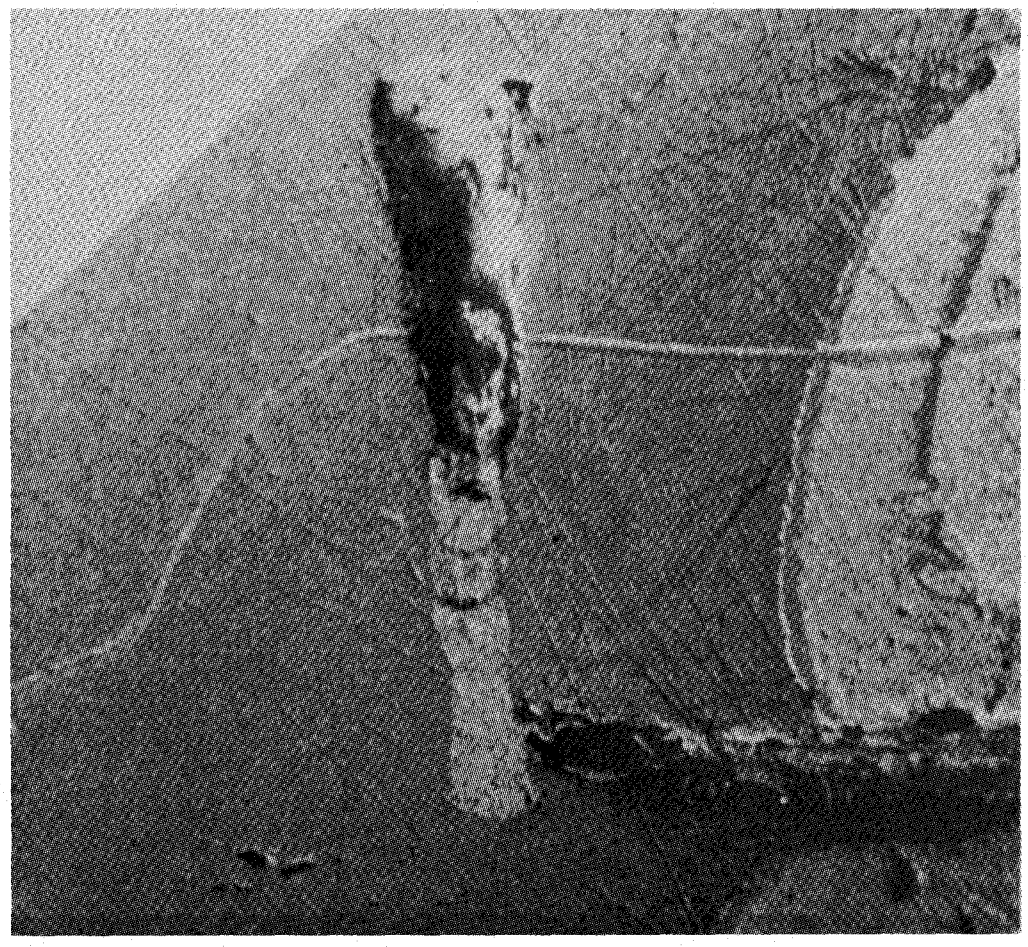

(b)

Fig. 10. (b) Taper lapped examination of the inset portion of Fig. 10(a), showing depth of damage under the gate entry area, same device.

There is as yet no discernible pattern to these effects. Certainly some device types are generally worse than others. There is no apparent correlation with measured $1/f$ noise or measured values of gate/source Schottky ideality factor n.

B. Interpulse Behavior

The recovery effects described above reveal behavior which is of less immediate importance to radar receiver performance than that of interpulse behavior. To study the latter, a special X-band interpulse test set has been commissioned, which permits simultaneous measurement of dynamic, interpulse gain and noise figure as well as dynamic return loss during pulses (Fig. 14). The noise figure is measured as the average value within any selectable 20-μs "window" located within the interpulse duration. Due to the choice of frequencies for the pulse source, gain and noise measurement paths and to the incorporation of suitable filters, the interaction between the different signals is avoided, as are paralysis effects in the various components. The TWTA permits short term catastrophic burnout investigations up to pulse levels at least as high as those corresponding to unprimed protection units, and the all solid-state pulse source provides a versatile method of generating RF spike, flat-topped, or spike plus flat-topped pulse trains having very low statistical variation in power level. Furthermore, exposure testing can be undertaken on a one-shot basis as well as continuously. Initial results are shown in Fig. 15 and show significant difference between a good device and poor device; the noise figure has deliberately not been corrected for second stage contribution here.

VI. Conclusions

Catastrophic burnout energies have been reported for various types of available low-noise GaAs MESFET's. The wide variation in levels does not appear to correspond to any measurable parameter. Further work on this is underway, including the use of predosage low-current SEM examination; further angle-lapping examinations calculation of the current and field waveforms in the channel; and measurement by sampling scope of the actual current waveform during pulsing and its relationship to bias. Preliminary longer term lower energy tests suggest some caution in relation to the reliability of the devices in radar receivers, an experience understandably similar to that

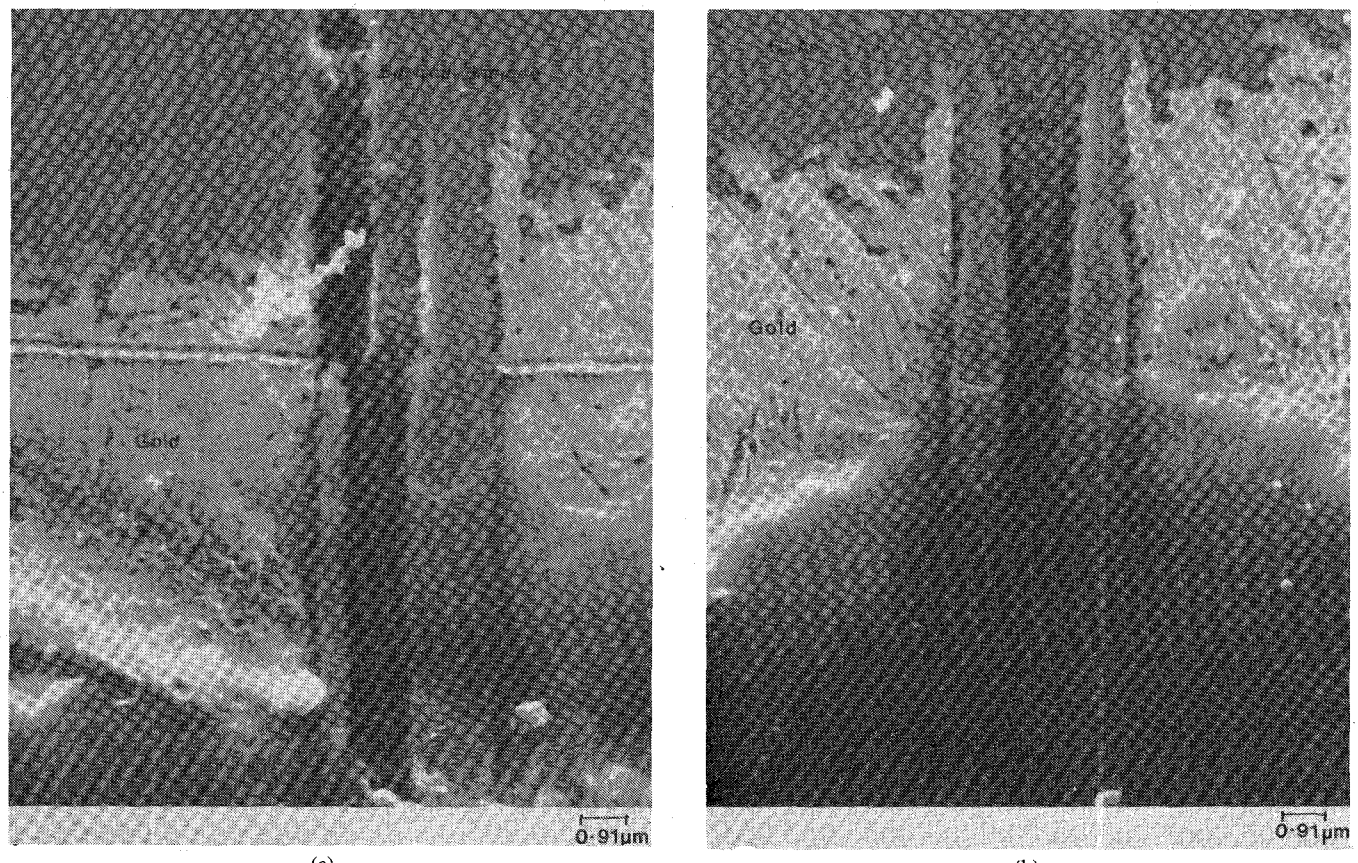

(a) (b)

Fig. 11. (a) Taper lapped examination of gate/source failure, showing depth of damage in epilayer. (b) Taper lapped examination of gate structure of good section of same device.

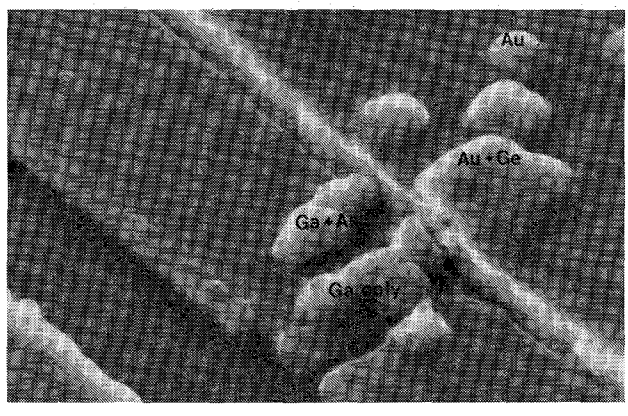

Fig. 12. EDAX examination of drain edge. Area shown is further along gate stripe of same device as Fig. 9.

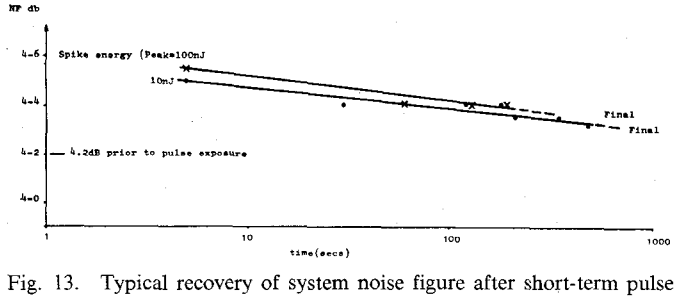

Fig. 13. Typical recovery of system noise figure after short-term pulse exposure.

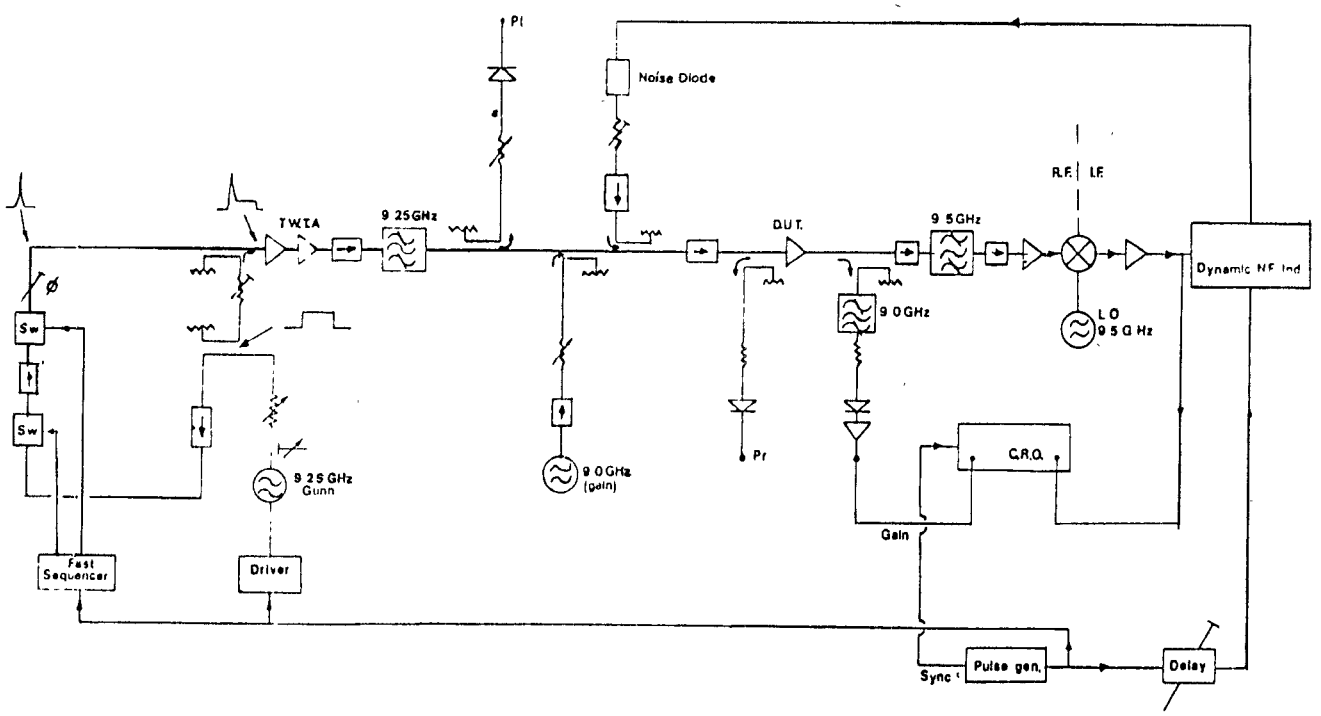

Fig. 14. Interpulse test set block diagram.

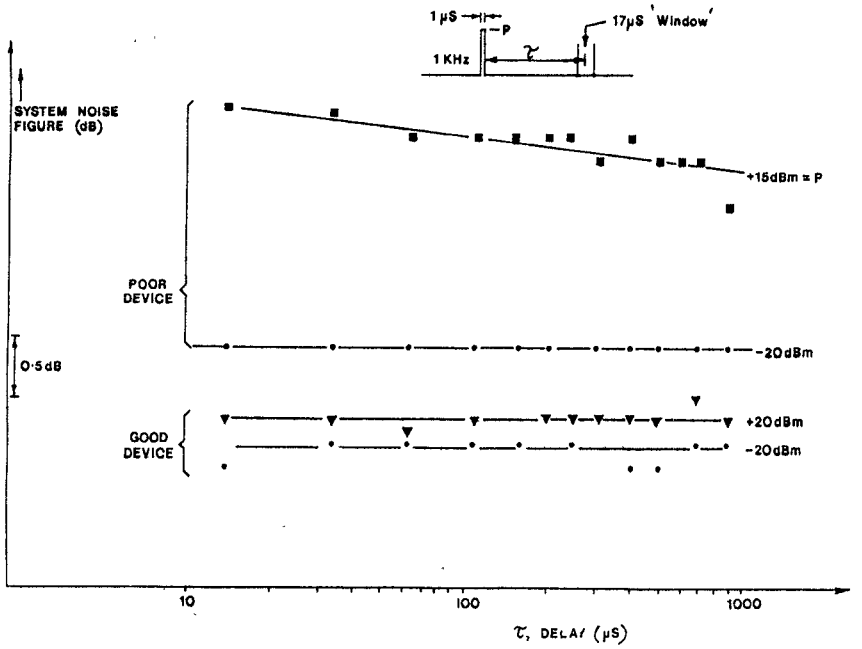

Fig. 15. Interpulse noise figure behavior. The center of the measurement "window" is τ μs nom. from the end of pulse. Pulse is of power level P.

encountered with mixer diodes.

Noncatastrophic recoverable effects have been observed, with many devices exhibiting annealing effects at relatively low energy dosage. Further work is underway on interpulse testing, using the test set described. It is particularly necessary to isolate the gain and noise figure components of the devices from any measured changes in overall system noise figure. Again, the effects observed are not understood at present, and it is similarly desirable to determine some correlation with other measurable device or processing characteristics.

Acknowledgment

The authors are indebted to R. Murray of Ferranti Professional Components Department, Dundee, Scotland, S. Simmens of the Shirley Institute, Manchester, England,

and to P. Martin, K. Broome, and M. Appleby for their assistance.

REFERENCES

[1] J. J. Whalen, M. Thorn, and M. C. Calcatera, "Microwave nanosecond pulse burn out properties of GaAs MESFETS," in *MTT-S Int. Microwave Symp. Proc.*, Orlando, FL, May 1979.
[2] J. J. Whalen, M. C. Calcatera, and M. L. Thorn, "Microwave nanosecond pulse burn out properties of GaAs MESFETS," *IEEE Trans. Microwave Theory Tech.*, vol. MTT-27, pp. 1026–1031, Dec. 1979.
[3] T. Suzuki, M. Otsubo, T. Ishii, and K. Shirahata, "Study on reliability of low noise GaAs MESFET's," in *Ninth European Microwave Conf. Proc.* pp. 331–337, Brighton, Sept. 1979.
[4] J. Arnold, "Ruggedised GaAs FET amplifiers for military applications," in *Proc. Military Microwave Conf.*, London, pp. 651–656, Oct. 1980.

✤

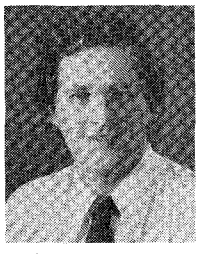

David S. James (M'71) was born in Bradford-on-Avon, England, on January 24, 1945. He recieved the B.Sc. and Ph.D. degrees in electonics engineering from the University College of North Wales, Bangor, U.K.

From 1970 to 1977, he was employed by the Department of Communications, Communications Research Centre, Ottawa, Ont., Canada. He is now with Ferranti Ltd., Manchester, U.K. His work involves the development of passive and solid-state microwave circuits, especially low-noise satellite subsystems.

Dr. James was Chairman of the Ottawa X-MTT Chapter and is a member of the A. V.S. and the IEE (UK).

✤

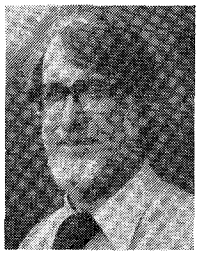

Leslie Dormer was born in Manchester, England, on November 23, 1930. He was educated up to Higher National Certificate level in chemistry at Stockport College and John Dalton College, Manchester.

After five years in Textile Research, he became a Fuel Technologist working for Hawker Siddeley Dynamics from 1962–1967. In February 1967, he joined Ferranti Ltd. as a Chemist in the semiconductor facility, in which position he developed an interest in microwave parametric amplifier production. During the early years in the semiconductor facility he was awarded patents for metallization processes. In April 1973, he became Chief Chemist for Ferranti Electronics Ltd. and has since become actively involved in sponsored research into problems associated with semiconductor devices as used in solid-state microwave equipment.

Horn Image-Guide Leaky-Wave Antenna

TRANG N. TRINH, STUDENT MEMBER, IEEE, RAJ MITTRA, FELLOW, IEEE, AND ROY J. PALETA, JR.

***Abstract*—A novel structure for a frequency-scanning millimeter-wave antenna is described. The antenna is constructed by embedding a dielectric leaky-wave antenna in a long trough with metal flares attached along both sides. The optimum flare angle for achieving maximum gain is theoretically predicted. The design of the leaky-wave antenna, which is comprised of metallic-strip perturbations on top of the dielectric guide, is also discussed.**

Manuscript received April 13, 1981; revised August 6, 1981.

T. N. Trinh and R. Mittra are with the Department of Electrical Engineering, University of Illinois, Urbana, IL 61801.

R. J. Paleta, Jr., is with the Harris Corporation, T.S.T.O. 24/2455, Melbourne, FL 32901.

I. INTRODUCTION

RECENT TRENDS toward the use of low-cost, high-resolution antennas for short-range communications have encouraged the design and development of different millimeter-wave antennas [1]–[4]. The leaky-wave antenna

0018-9480/81/1200-1310$00.75 ©1981 IEEE